Molecular Microbiology (2004) **53**(2), 419–432 doi:10.1111/j.1365-2958.2004.04133.x

Structural analysis of the chromosome segregation protein Spo0J from *Thermus thermophilus*

Thomas A. Leonard,* P. Jonathan G. Butler and Jan Löwe
MRC Laboratory of Molecular Biology, Hills Road, Cambridge CB2 2QH, UK.

Summary

Prokaryotic chromosomes and plasmids encode partitioning systems that are required for DNA segregation at cell division. The plasmid partitioning loci encode two proteins, ParA and ParB, and a *cis*-acting centromere-like site denoted *parS.* The chromosomally encoded homologues of ParA and ParB, Soj and Spo0J, play an active role in chromosome segregation during bacterial cell division and sporulation. Spo0J is a DNA-binding protein that binds to *parS* sites *in vivo.* We have solved the X-ray crystal structure of a C-terminally truncated Spo0J (amino acids 1–222) from *Thermus thermophilus* to 2.3 Å resolution by multiwavelength anomalous dispersion. It is a DNA-binding protein with structural similarity to the helix–turn–helix (HTH) motif of the lambda repressor DNA-binding domain. The crystal structure is an antiparallel dimer with the recognition α-helices of the HTH motifs of each monomer separated by a distance of 34 Å corresponding to the length of the helical repeat of B-DNA. Sedimentation velocity and equilibrium ultracentrifugation studies show that full-length Spo0J exists in a monomer–dimer equilibrium in solution and that Spo0J1–222 is exclusively monomeric. Sedimentation of the C-terminal domain of Spo0J shows it to be exclusively dimeric, confirming that the C-terminus is the primary dimerization domain. We hypothesize that the C-terminus mediates dimerization of Spo0J, thereby effectively increasing the local concentration of the N-termini, which most probably dimerize, as shown by our structure, upon binding to a cognate *parS* site.

Introduction

The segregation of newly replicated chromosomes of eukaryotic cells is mediated by a microtubule-based spindle that pulls chromosomes to opposite sides of the cell before cytokinesis (Heald, 2000; Sharp *et al*., 2000). In contrast, the nature of the machinery that ensures faithful segregation of DNA is obscure for prokaryotes. Early models (Jacob *et al*., 1963) postulate the coupling of replicating DNA to the elongating cellular envelope as instrumental in bacterial DNA segregation. However, zonal growth is not a general feature of cell wall growth and, therefore, it is unlikely that this model explains the segregation of newly replicated chromosomes (Mobley *et al*., 1984). More recently, it was discovered that DNA replication in *Escherichia coli* and *Bacillus subtilis* takes place at a centrally located replication factory (Lemon and Grossman, 1998; Koppes *et al*., 1999). This led to the proposal of a 'factory model' for chromosome segregation: bidirectional extrusion of replicated DNA from the replication factory followed by condensation intrinsically segregates sister nucleoids (Lemon and Grossman, 1998; 2000; 2001; Koppes *et al*., 1999; Gordon and Wright, 2000; Sawitzke and Austin, 2001; Onogi *et al*., 2002). A third model has emerged from fluorescence microscopy experiments, which indicate that replicated plasmids (Gordon *et al*., 1997; Niki and Hiraga, 1997; Jensen and Gerdes, 1999) and chromosomal origins of replication (Lewis and Errington, 1997; Webb *et al*., 1997; 1998; Niki and Hiraga, 1998; Jensen and Shapiro, 1999; Niki *et al*., 2000) move rapidly from mid-cell to fixed positions near the cell poles or at one-quarter and three-quarters of cell length (Sharpe and Errington, 1999; Hiraga, 2000; Moller-Jensen *et al*., 2000), suggesting the existence of a prokaryotic mitosis-like apparatus. In this sense, the prokaryotic origin-proximal region seems to be a counterpart of eukaryotic centromeres (Wheeler and Shapiro, 1997). Most recently, RNA polymerase has emerged as a novel candidate for driving the poleward segregation of bacterial chromosomes (Dworkin and Losick, 2002).

Partitioning determinants, or the *par* genes, are critical components of DNA segregation. The *par* genes were originally identified from studies of low-copy-number plasmids and are referred to as the *parAB* family. Partitioning modules confer genetic stability upon their replicons through specific subcellular positioning of the DNA (Gordon *et al*., 1997; Niki and Hiraga, 1997; Jensen and Gerdes, 1999). Generally, *par* systems are composed of three essential components: (i) an ATPase and (ii) a protein that

Accepted 17 March, 2004. *For correspondence. E-mail tleonard@mrc-lmb.cam.ac.uk; Tel. (+44) 1223 252 969; Fax (+44) 1223 213 556.

binds to (iii) one or more *cis*-acting, centromere-like DNA regions. The *par* genes of the *E. coli* plasmids F (*sopABC*) (Niki and Hiraga, 1997), R1 (*parMRC*) (Gerdes *et al*., 2000) and P1 (*parABS*) (Austin and Abeles, 1983a,b) are required for accurate plasmid partitioning. It should be noted, however, that ParM of plasmid R1 is not, in fact, a ParA homologue like SopA but a member of the actin family of ATPases (van den Ent *et al*., 2002). ParB of plasmid P1 binds to a *cis*-acting site, *par*S, and forms a large nucleoprotein complex in conjunction with ParA, which is an ATPase (Bouet *et al*., 2000). ParB has also been shown to be capable of pairing P1 centromere-like *parS* sites (Edgar *et al*., 2001).

The notion of plasmids containing partitioning determinants essential for their stable inheritance was extended to bacterial chromosomes by the identification of *par* genes in bacterial genomes by sequence homology searches. The *par* operon was subsequently identified in the *ori*C region of a subset of bacterial genomes; it consists of two transacting genes, *soj* and *spo0J*, and a *cis*-acting sequence, *parS*. More than 50 homologues of SopA and Soj (ParA) or SopB and Spo0J (ParB) have been identified in bacteria so far (Yamaichi and Niki, 2000).

Null mutants of Spo0J are lethal in *Caulobacter crescentus* (Mohl *et al*., 2001), and mutations in *spo0J* in *B. subtilis* result in the formation of anucleate cells (Ireton *et al*., 1994). Spo0J mutants of *B. subtilis* and *Pseudomonas aeruginosa* are viable but display perceptible defects in chromosome segregation in both vegetative and sporulating cells (Ireton *et al*., 1994; Sharpe and Errington, 1996; Godfrin-Estevenon *et al*., 2002; Lewis *et al*., 2002). Identification and characterization of a bacterial chromosome partitioning site revealed 10 pseudopalindromic 16 bp sequences found in the origin-proximal 20% of the *B. subtilis* chromosome (Lin and Grossman, 1998). Eight of the 10 sequences identified were shown to be bound by Spo0J *in vivo*, and the presence of one such site on an otherwise unstable plasmid stabilized the plasmid in a Soj- and Spo0J-dependent manner, demonstrating that the site, *parS*, can function as a partitioning site (Lin and Grossman, 1998). Moreover, it was later demonstrated that both the *B. subtilis* and the *P. aeruginosa* partitioning machineries can function in *E. coli* (Yamaichi and Niki, 2000; Godfrin-Estevenon *et al*., 2002). This promiscuity suggests that whatever host proteins interact with Soj and Spo0J are highly conserved. The 16 bp *parS* sites identified in *B. subtilis* have since been identified in other bacterial species including *P. aeruginosa* and *Pseudomonas putida* (Godfrin-Estevenon *et al*., 2002) and *Thermus thermophilus* (Nardmann and Messer, 2000). Most recently, a putative chromosomal partitioning site, *migS*, has also been identified in *E. coli* (Yamaichi and Niki, 2004). The consensus sequence 5′-tGTTTCACGT GAAACa-3′ shows a dyad symmetry typical of dimeric DNA-binding proteins. The half-palindromes of these sequences (tGTTTCAC, GTGAAACa) are similar to ParB box A motifs of P1 plasmid centromeres (e.g. A1, ATTTCAC; A3, GTGAAAT; Bouet *et al*., 2000; Surtees and Funnell, 2001). The only structural information about the ParB family of proteins to date has been the published crystal structure of the dimerization domain of KorB (Delbruck *et al*., 2002). The structure shows that the C-terminal 62 amino acids of KorB form a dimer, and cross-linking studies suggest that the C-terminal domain is responsible for stabilizing the KorB dimer in solution to facilitate binding to its cognate palindromic operator sequences (Delbruck *et al*., 2002).

In this study, we have solved the crystal structure of truncated Spo0J from the Gram-negative bacterium *T. thermophilus* to 2.3 Å resolution. The crystal structure is of Spo0J with 47 amino acids removed from the C-terminus as we were unable to obtain crystals of a full-length Spo0J. It is a tight dimer with high α-helical content and contains a putative helix–turn–helix (HTH) DNA-binding motif in each monomer. We show that Spo0J of *T. thermophilus* is able to bind DNA containing a *parS* site. The structure of Spo0J is the first structure to be reported of the DNA-binding domain from this ubiquitous and highly conserved family of ParB proteins, which have a central role in plasmid and chromosome segregation in prokaryotes. Based on this structure and the structure of the C-terminal domain of KorB (Delbruck *et al*., 2002), together with ultracentrifugation analysis, we propose that Spo0J contains a C-terminally located primary dimerization domain and an N-terminally located secondary dimerization domain, which brings the HTH motifs of the antiparallel dimer into register for DNA binding. We show that the C-terminus of Spo0J is necessary for extensive binding to plasmid DNA, and we speculate that it plays a role in spreading along DNA.

Results

Cloning and protein purification

Spo0J was cloned and the protein overexpressed and purified from nine bacterial genomes but failed to crystallize in all cases. The proteins all displayed low precipitation (<2% of 1152 conditions) and abundant phase separation. The C-terminal regions of these proteins have the weakest homology to each other, and so a series of C-terminal truncated proteins was overexpressed in an attempt to grow crystals. The *spo0J1–666* gene from *T. thermophilus* encoding residues 1–222 of 269 amino acids found in the full-length protein was cloned and overexpressed according to the protocol detailed in *Experimental procedures*.

DNA-binding activity

Gel retardation assays of Spo0J from *T. thermophilus* and *Bacillus stearothermophilus* were performed to confirm DNA-binding activity for these previously uncharacterized members of the Spo0J family. Sequence alignment with Spo0J of *B. subtilis* confirmed that this protein was almost certainly a Spo0J homologue (42% sequence identity) (Fig. 6). Both proteins are able to bind *in vitro* a 16 bp duplex containing the pseudopalindromic *parS* sequence 5′-TGTTCCACGTGAAACA-3′ (Fig. 1A and B). To test for the ability of wild-type and truncated proteins to carry out DNA binding and spreading, we used an agarose gel shift assay developed by H. Ferreira and J. Errington (unpublished). Gel retardation assays using a pUC19 derivative plasmid, pUOJ (see *Experimental procedures*), containing a single *parS* site show that *T. thermophilus* Spo0J is also able to shift a 2938 bp supercoiled plasmid *in vitro*. Incubation of the target DNA with increasing amounts of Spo0J results in differential, stepwise shifting of the DNA to higher positions in the gel, with the migration of a maximally shifted band indicative of saturation of the DNA with protein. Calculation of the ratio of Spo0J molarity to approximated binding site molarity confirms an approximate coating of the DNA at saturating protein concentration (assuming that the protein physically covers a binding site of 24 bp). The differential retardation of plasmid DNA by Spo0J indicates that the protein is able to bind DNA non-specifically with high affinity. Gel retardation of pUOJ by Spo0J1–222 shows that the supershifting of plasmid DNA by full-length Spo0J is dependent on the presence of the C-terminal domain (Fig. 1C). It is possible to gel filtrate a stable complex of full-length Spo0J with 16–24 bp oligonucleotides of *parS* DNA, but not possible with the C-terminal deletion mutant, Spo0J 1–222 (data not shown). The binding of Spo0J to DNA is clearly weakened, if not abrogated by removal of the C-terminus.

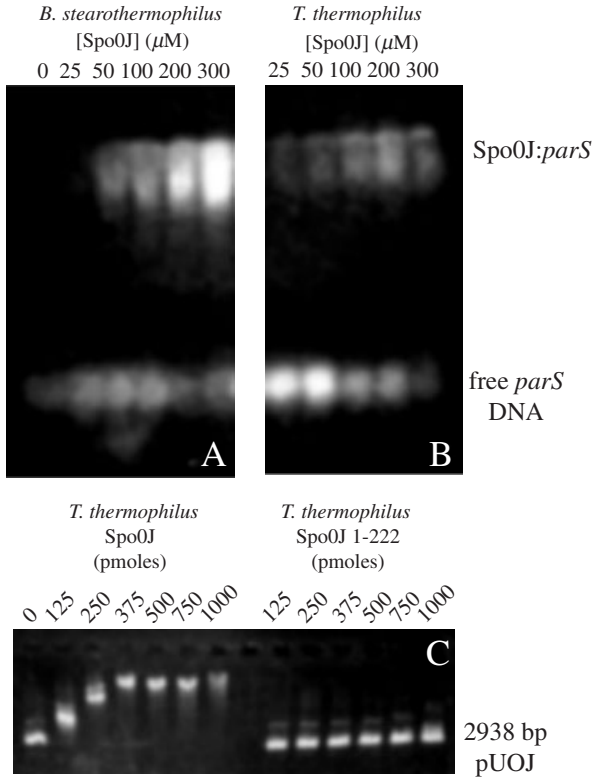

Fig. 1. DNA binding by Spo0J *in vitro*.
A. Gel retardation assay illustrating *parS* binding by Spo0J of *Bacillus stearothermophilus*. At the highest concentration of Spo0J, almost all the DNA is bound.
B. DNA binding by Spo0J of *T. thermophilus*. The result provides clear evidence that this protein also has the expected DNA-binding activity.
C. Gel retardation of plasmid DNA (2938 bp) by *T. Thermophilus* Spo0J. Saturation of the DNA occurs at an approximate equimolar concentration of 24 bp binding sites to dimeric Spo0J (full length). Spo0J 1–222, which has the C-terminal domain removed, is incapable of shifting plasmid DNA.

Crystallization and structure determination

SeMet-substituted protein was produced in the non-methionine auxotrophic C41(DE3) cells (Van Duyne *et al.*, 1993). Crystals belong to space group C222, and the phase problem was solved using multiwavelength anomalous dispersion (MAD) with one crystal containing SeMet-substituted protein at 3.0 Å resolution. Crystallographic data are summarized in Table 1. Eight NCS-related molecules were built, and the phases were

Table 1. Crystallographic data.

Crystal	λ (Å)	Resol. (Å)	$I/\sigma I$[a]	R_m[b] (%)	Multipl.[c]	Compl.[d] (%)
PEAK	0.9791	2.6	6.7	0.064	12.2 (6.1)	99.1 (97.9)
INFL	0.9793	2.6	4.3	0.068	12.2 (6.1)	99.8 (98.0)
HREM	0.9393	2.6	2.3	0.080	12.0 (6.0)	99.8 (97.5)
NATI	0.9393	2.3	3.0	0.078	3.5	98.3

a. Signal-to-noise ratio for the highest resolution of intensities.
b. R_m: $\Sigma_h\Sigma_l|I(h,l)-I(h)|/\Sigma_h\Sigma_l I(h,l)$ where $I(h,l)$ are symmetry-related intensities, and $I(h)$ is the mean intensity of the reflection with unique index h.
c. Multiplicity for unique reflections, anomalous multiplicity in brackets.
d. Completeness for unique reflections, anomalous completeness in brackets.
Space group C222 (21), a = 182.24 Å, b = 295.15 Å, c = 73.49 Å.

Table 2. Refinement statistics.

Model	Chains A–H, residues 23–209
Diffraction data	NATI, 2.3 Å, all data
R-factor, *R*-free[a]	0.2354, 0.2780
B average/bonded[b]	39.39 Å^2/3.52 Å^2
Geometry bonds/angles[c]	0.006 Å/1.2
Ramachandran[d]	97.3%/0.0%
PDB ID[e]	1vz0

a. Five per cent of reflections were randomly selected for determination of the free *R*-factor, before any refinement.
b. Temperature factors averaged for all atoms and r.m.s.ds of temperature factors between bonded atoms.
c. R.m.s.ds from ideal geometry for bond lengths and restraint angles (Engh, 1991).
d. Percentage of residues in the 'most favoured' region of the Ramachandran plot and percentage of outliers (PROCHECK; Laskowski *et al*., 1993).
e. Protein Data Bank identifiers for co-ordinates and structure factors respectively.

extended to 2.3 Å using eightfold non-crystallographic symmetry (NCS). A model was built for residues 23–209 for chains A–H and refined to an *R*-factor of 24.3 and a free *R*-factor of 29.2 (Table 2).

Spo0J monomer structure

Spo0J is a compact structure of 65% α-helical content. There was no electron density for residues Met-1–Gly-22 or residues Arg-210–Glu-222. The N-terminal region, residues Val-23–Lys-97, consists of a long α-helix, H2, followed by a short three-stranded β-sheet with strands S2 and S3 separated by a short α-helix H3. Strands S1 and S2 form an antiparallel sheet with strand S3 running parallel to the central strand S1. The remainder of the monomer is all α-helical with helices H6 and H7 forming a characteristic HTH motif. Helices H4–H11 form a compact α-helical domain in which helices H6, H7, H9 and H11 lie across the top of helices H4, H5, H8 and H10 (Fig. 2A). A three-dimensional similarity search using DALI (Holm and Sander, 1995) found Spo0J to be a novel protein structure with low homology to known protein structures. The closest known tertiary structure was that of a mitochondrial import receptor subunit fragment (PDB entry 1OM2), which gave a *Z*-score of just 4.9 and a root mean square deviation of Cα atoms of 2.8 Å. Later it was determined that, despite the novel overall fold of the protein,

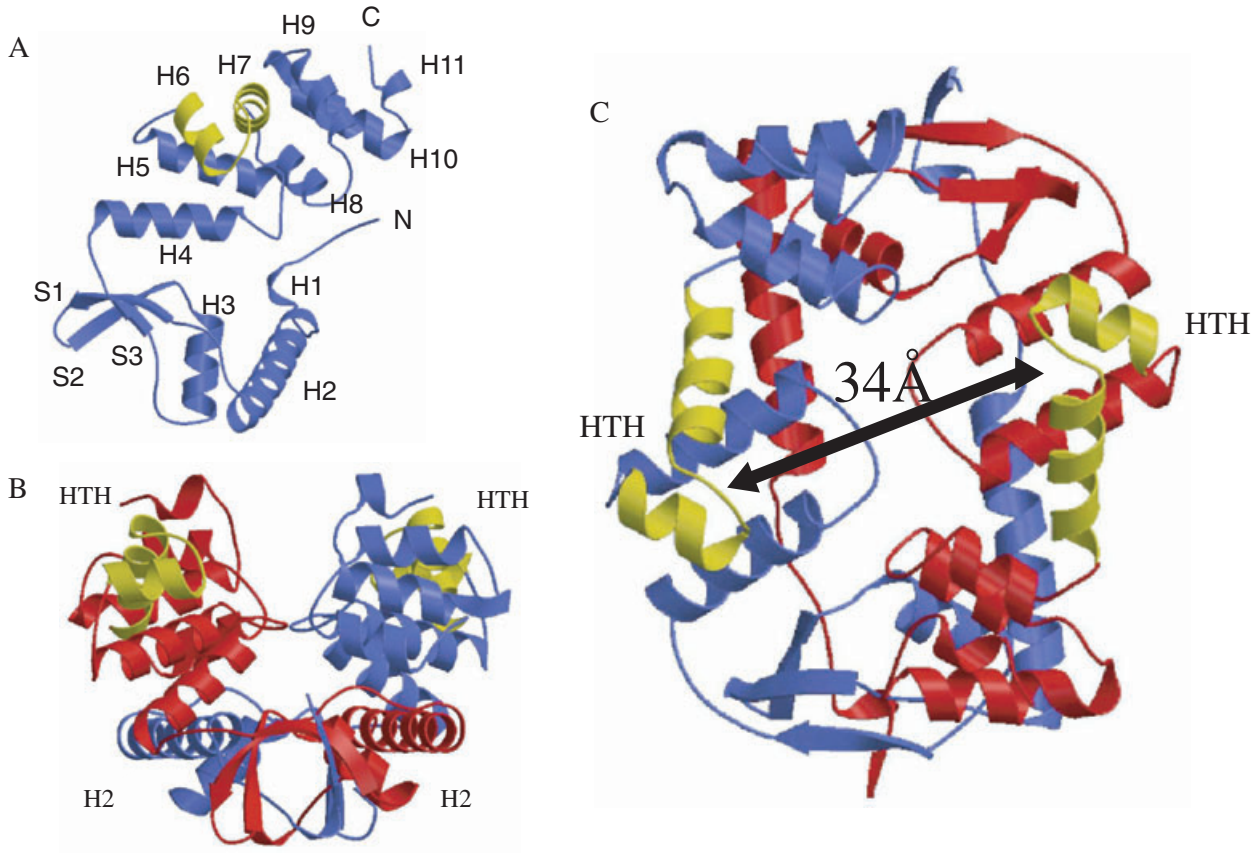

Fig. 2. Ribbon plots of (A) Spo0J monomer, (B) Spo0J dimer (end view) and (C) Spo0J dimer (top view). The HTH motifs are coloured yellow. The N-terminal α-helices forming the bulk of the dimer interface are indicated by H2. The distance between the HTH motifs in the dimer is 34 Å, corresponding to the helical repeat of B-DNA. The figure was prepared using the program MOLSCRIPT (Kraulis, 1991).

Spo0J contains structural similarity in its HTH motif to the DNA-binding domain of the lambda repressor.

Spo0J dimer structure

The asymmetric unit of the Spo0J crystals contains eight molecules arranged in four very clear equivalent dimers, consisting of chains A–H. The dimer interface is extensive in Spo0J. The surface areas of the two Spo0J monomers in the dimer are 12 936.2 Å^2 and 12 742.6 Å^2, and the surface area for both together in the dimer is 18 464.6 Å^2. The surface area buried at the dimer interface is 7214.26 Å^2, representing 28% of the surface area of one monomer. The dimer interface consists of two sets of hydrophobic interactions at either end of the dimer and an extensive electrostatic surface interaction between the N-terminal α-helix H2 and the external surface formed by helices H4, H5, H8 and H10. The arrangement of the two monomers in the dimer is such that the long N-terminal α-helix H2 of each monomer interdigitates with the globular domain of the other to form an antiparallel dimer (Figs 2B and 3A). Hydrophobic interactions between the extended N-terminal chain Val-23–Pro-33 (VVRLPLASIRP) of one monomer and the hydrophobic surface formed by strands S1 (LLVRP), S2 (GYELVA), S3 (VPAVV) and the C-terminal part of helix H3 (AALMAGL) of the other stabilize the dimer. Helices H4, H5, H8 and H10 form a highly negatively charged surface that interacts extensively with the overall positively charged surface produced by helix H2 and the extended chain linking helix H2 with strand S1.

Mode of DNA binding

Each dimer contains two HTH motifs, one from each monomer, at either end of the elongated molecule (Fig. 1B). The angle formed between helices H6 and H7 of the HTH motif is 59.4°. The distance between the HTH motifs is 36.50 Å between the C_α-carbons of A152 and 31.95 Å between the C_α-carbons of N153, giving an average distance of 34.23 Å. Many prokaryotic DNA-binding domains contain an HTH motif that recognizes and binds specific regulatory regions of DNA (Luscombe *et al.*, 2000). The two α-helices have the same relative orientation to each other and are connected by a loop region of similar structure in all DNA-binding HTH motifs. The DNA sequences to which these motifs bind are palindromic or pseudopalindromic in nature, especially at their ends. The palindromic nature of these sequences is important because it means that the two halves of each binding site are related by an approximate twofold symmetry axis. The HTH motif is traditionally defined as a 20-amino-acid segment of two α-helices inclined at ≈60° to each other connected by a four-residue β-turn, a configuration that is

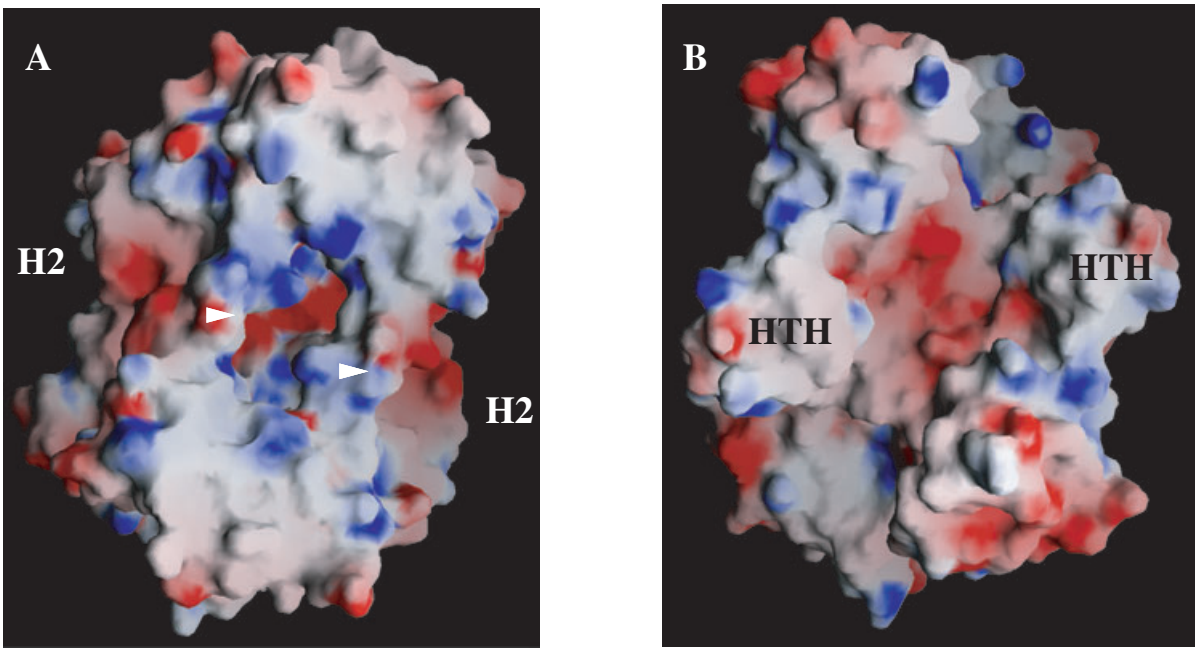

Fig. 3. Electrostatic surface potential plots of the Spo0J dimer.
A. View of the underside of the dimer.
B. The putative DNA-binding surface of the dimer (Fig. 3B is related to Fig. 2C by an ≈20° clockwise rotation). The helix–turn–helix motifs are indicated by HTH. The long N-terminal helix H2 of each monomer is shown in (A) forming the bulk of the dimer interface. Basic residues are coloured in blue and acidic residues in red. The figure was prepared using the program GRASP (Nicholls, 1993).

observed in the crystal structure of Spo0J. The definition can, however, be extended to those with longer linkers, such as loops, as long as the relative orientation of the α-helices is maintained (for example, the RAP1 protein family, PDB entry 1IGN; Konig *et al*., 1996).

The HTH motif invariably binds in the DNA major groove. The second α-helix is known as the recognition α-helix and is inserted in the groove. Although motifs from different protein families are structurally very similar (Suzuki *et al*., 1995), little homology is observed outside the motif. There is also little sequence similarity between the motifs of different families, and this variation allows them to recognize distinct sets of DNA sequences. However, a SUPERFAMILY (Gough *et al*., 2001) hidden Markov model search with *T. thermophilus* Spo0J indicates homology of the region Met-133–Leu-168 with the lambda repressor-like HTH DNA-binding domains. Met-133–Leu-168 maps exactly to the HTH motif of Spo0J in the crystal structure, indicating that there is a high likelihood that Spo0J is a genuine HTH DNA-binding protein. The X-ray structure of the N-terminal DNA-binding domain of the lambda repressor at 3.2 Å (Pabo and Lewis, 1982) shows the same arrangement of the helices of the HTH motif as is observed in the crystal structure of Spo0J. Seven residues in the 20-amino-acid HTH segment of Spo0J (Q137–R156) correspond to identical residues in the HTH segment of the lambda repressor (Q33–N52), representing 35% identity. The root mean square (r.m.s.) between Cα atoms in the two HTH motifs is 0.74 Å, and the mean distance between matching Cα atoms is 0.67 Å. The Cα traces of the two motifs are superimposed in Fig. 4. The

Table 3. Density increments and extinction coefficients.

	Spo0J	Spo0J1-222.
Solvent density	1.007068 g ml^{-1}	
Solution density	1.009666 g ml^{-1}	1.008302 g ml^{-1}
Protein concentration	9.69 mg ml^{-1}	4.96 mg ml^{-1}
Density increment	0.268	0.249
Apparent specific volume (ϕ')	0.727 ml g^{-1}	0.746 ml g^{-1}
ε_{280}	1.81×10^4 M^{-1}	1.04×10^4 M^{-1}
ε_{230}	2.04×10^5 M^{-1}	9.02×10^4 M^{-1}

subunit interactions in lambda repressor and Spo0J have an important consequence in that they cause the second α-helix in the HTH motifs of each subunit to be at opposite ends of the elongated dimeric molecule, separated by a distance of 34 Å. This distance corresponds almost exactly to one helical turn of a B-DNA double helix. As a result, the recognition α-helices of the two subunits can bind into successive major grooves of a DNA molecule. The structural homology of the Spo0J HTH motif with the known DNA-binding HTH motif of lambda repressor, coupled with the distance measurements between the HTH motifs in the two crystal structures, makes a strong case for Spo0J binding to *parS* sites in this manner.

Analytical ultracentrifugation of Spo0J

Density increments and extinction coefficients. Density increments and extinction coefficients of solutions of Spo0J and truncated Spo0J were calculated from the measured densities, spectra and protein concentrations, as shown in Table 3.

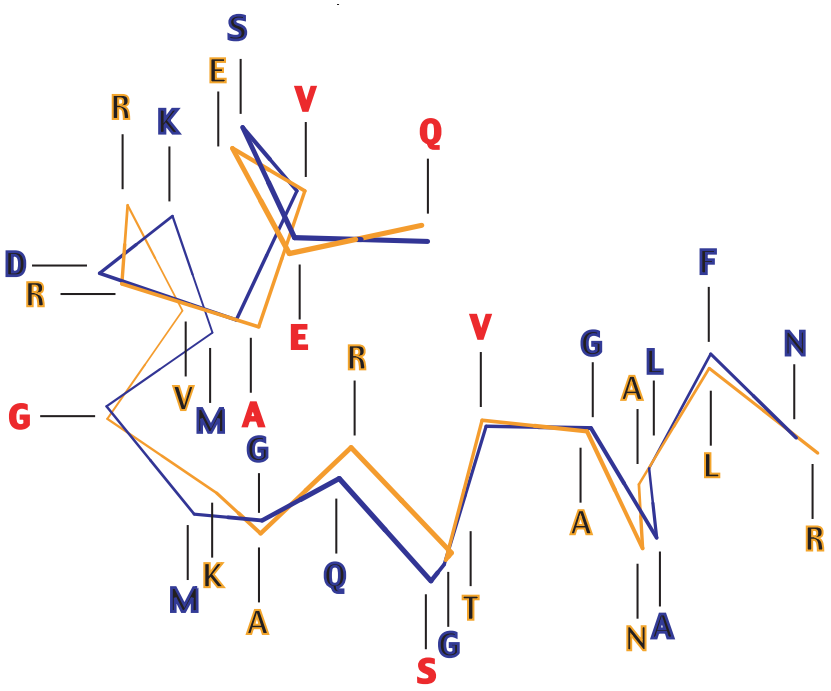

Fig. 4. Backbone Cα trace of the HTH motif of Spo0J superimposed on a backbone trace of the lambda repressor HTH motif. The lambda repressor HTH structure is coloured blue, and the Spo0J HTH structure is coloured orange. The r.m.s.d. between the two Cα structures is 0.74 A. Identical residues in the two motifs are marked red. Despite the lack of sequence similarity, the motifs display high structural homology, comprising two helices oriented at 60° to each other separated by a four-residue β-turn. The figure was prepared using the program MOLSCRIPT (Kraulis, 1991).

Molecular mass

After sedimentation equilibrium, the weight-averaged, apparent molecular mass was plotted against concentration (Fig. 5). For full-length Spo0J, these plots appeared to correspond to a monomer/dimer equilibrium, with negligible evidence of any non-ideality (Fig. 5A). Moreover, plots from different loading concentrations overlie each other closely enough to suggest that the aggregation is fully reversible. The original data were therefore fitted with

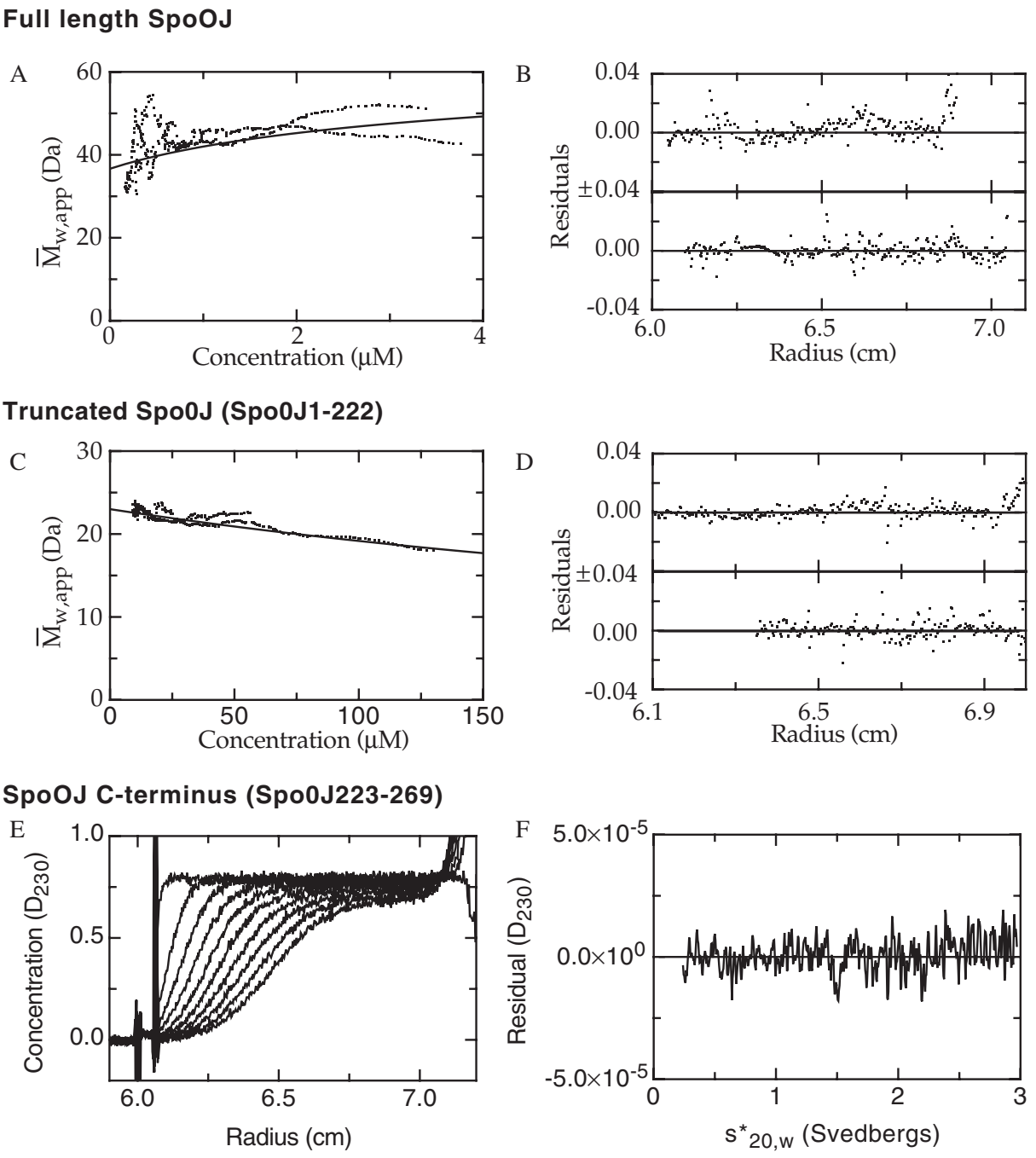

Fig. 5. Plots of $\overline{M}_{w,app}$ against concentration for Spo0J and truncated Spo0J (left) and of the residuals for fitting as monomer/dimer equilibrium and non-ideal monomer respectively (right). Points are for individual datum points from the equilibrium scans; lines (on left) are calculated theoretically taking M_1 = 36 500 Da and K_D = 10 μM (full-length Spo0J) and M_1 = 22 600 Da and B = 1525 M^{-1} (SpoOJ 1–222). Plots of scans during the sedimentation velocity run with Spo0J 223–269 (bottom). Plots of individual scans at 2.5 min intervals are shown on the left, and a plot of the residuals against $s^*_{20,w}$, for fitting scans 81–92, on the right, to show the good fit to a single component, corresponding to $s_{20,w}$ = 1.43 (±0.005) S and Mr = 13.7 (±0.25) kDa.

the equation for such aggregation. Typical plots of the resulting residuals are shown (Fig. 5B), showing that this is an appropriate model. The best estimate for the monomer mass is 36 (±6) kDa. The fit also gave a best estimate for K_d of 10 (±3) μM. These estimates were used to plot a fitted curve on to the plot of weight-averaged, apparent molecular mass against concentration (Fig. 5).

For the Spo0J1–222, the plots appeared to correspond to a non-ideal monomer. The original data were therefore fitted with the equation for this, and the resulting residuals are shown (Fig. 5D), showing that this is an appropriate model. The fit gave best estimates of the monomer mass as 23 (±0.25) kDa and the second osmotic virial coefficient (B) of 1000 (±100) M^{-1}. These estimates were again used to plot a fitted curve on to the plot of weight-averaged, apparent molecular mass against concentration (Fig. 5C).

The C-terminal fragment (Spo0J 223–269) was examined by sedimentation velocity and gave a well-shaped, symmetrical boundary (Fig. 5E). The data were analysed using the dc/dt analysis (Stafford, 1994; 1997; Philo, 2000). Groups of 12 scans were taken shortly after the boundary cleared the meniscus, in the middle of the run and towards the end of the run. In each case, the data were well fitted by a single component, with a mean sedimentation coefficient of 1.48 S and a molecular mass of 12.3 kDa. This corresponds well to a dimer of the protein (M1 = 6.05 kDa). The residuals confirm that the data is well fitted by a single dimeric species (Fig. 5F). We therefore conclude that the C-terminal region of Spo0J dimerizes strongly, while the DNA-binding domain (Spo0J 1–222) on its own tends to remain monomeric. The overall protein thus dimerizes with an intermediate K_d of ≈10 μM.

Discussion

At present, the exact function of Spo0J is ambiguous. From the structure, it appears that Spo0J is a classical prokaryotic HTH DNA binding protein in which the antiparallel dimer forms a central DNA-binding domain containing two HTH motifs separated by the helical repeat of B-DNA. Comparison of the HTH motif with that of the lambda repressor provides further evidence for this mode of DNA binding.

Genetic studies on Spo0J of *B. subtilis* have identified a number of mutations that correlate with a defect in chromosome segregation (Autret *et al*., 2001). These mutations were made on the basis of conservation of particular residues between Spo0J and the ParB proteins. Six point mutations were identified that gave rise to abnormal nucleoid appearance with substantial numbers of elongated cells containing uncondensed nucleoids and a few anucleate cells. Only mutation R148A maps to the HTH motif in the crystal structure of *T. thermophilus* Spo0J, and binding studies by electrophoretic mobility shift assay (EMSA) have not been performed on this mutant. The mutations F42A, R80A, E106G, N112A and R206C most probably represent folding mutations or mutations that abrogate protein–protein interactions essential in the partitioning complex.

Our structure is the first structure of the DNA-binding domain of a Spo0J/ParB protein to be solved. The dimerization domain of the homologous protein KorB (PDB entry 1IGQ) from plasmid RP4 has already been solved (Delbruck *et al*., 2002), which means that we now have structural information on both parts of the protein. KorB is a regulatory protein encoded by the conjugative plasmid RP4, which controls the expression of plasmid genes involved in replication, transfer and stable inheritance of RP4 DNA. Like *B. subtilis* Spo0J, RP4 KorB binds to palindromic DNA sequences present 12 times in the 60 kb plasmid (Balzer *et al*., 1992). In the phylogenetic trees, KorB clusters with the chromosomally encoded members of the ParB family and away from the plasmid-encoded homologues (Hayes, 2000). The C-terminal 62 residues of KorB (Lys-297–Gly-358) present in the structure align with the C-terminal 47 amino acids missing in our structure of *T. thermophilus* Spo0J (Spo0J223–269) (Fig. 6). The C-terminal portion of KorB is a globular domain comprising a five-stranded antiparallel β-barrel with a structure similar to that of Src homology 3 (SH3) domains. The domain was observed crystallographically as a dimer with a predominantly hydrophobic subunit interface formed by a leucine zipper-like arrangement. By chemical cross-linking experiments, it was demonstrated that KorB–C forms dimers in solution as well. Functional dissection of KorB from plasmid RK2 (100% sequence identity to KorB of plasmid RP4) identifies the C-terminus as the primary dimerization domain. Classical HTH DNA-binding proteins such as the Trp repressor, λ Cro and *E. coli* catabolite gene regulator protein (CRP) must be dimeric in order to bind the DNA efficiently (Pabo and Sauer, 1992), suggesting that C-terminal deletion mutants of KorB are still able to bind DNA in their dimeric form. The crystal structure of Spo0J clearly illustrates the ability of the N-terminal domain to dimerize, albeit at the high protein concentrations that favour crystallization. This N-terminal dimer is most probably physiologically relevant because it brings the two HTH motifs into the required context for binding to DNA. To investigate dimer formation further, we have shown by analytical ultracentrifugation (Fig. 5) that full-length Spo0J exists as a monomer–dimer equilibrium in solution with a K_d of 10 (±3) μM, but that the C-terminally truncated protein that we have solved the crystal structure of is exclusively monomeric in solution, indicating that another determinant is required for dimerization in solution. There are two possibilities: one involves dimerization of the full-length protein mediated by the C-terminus,

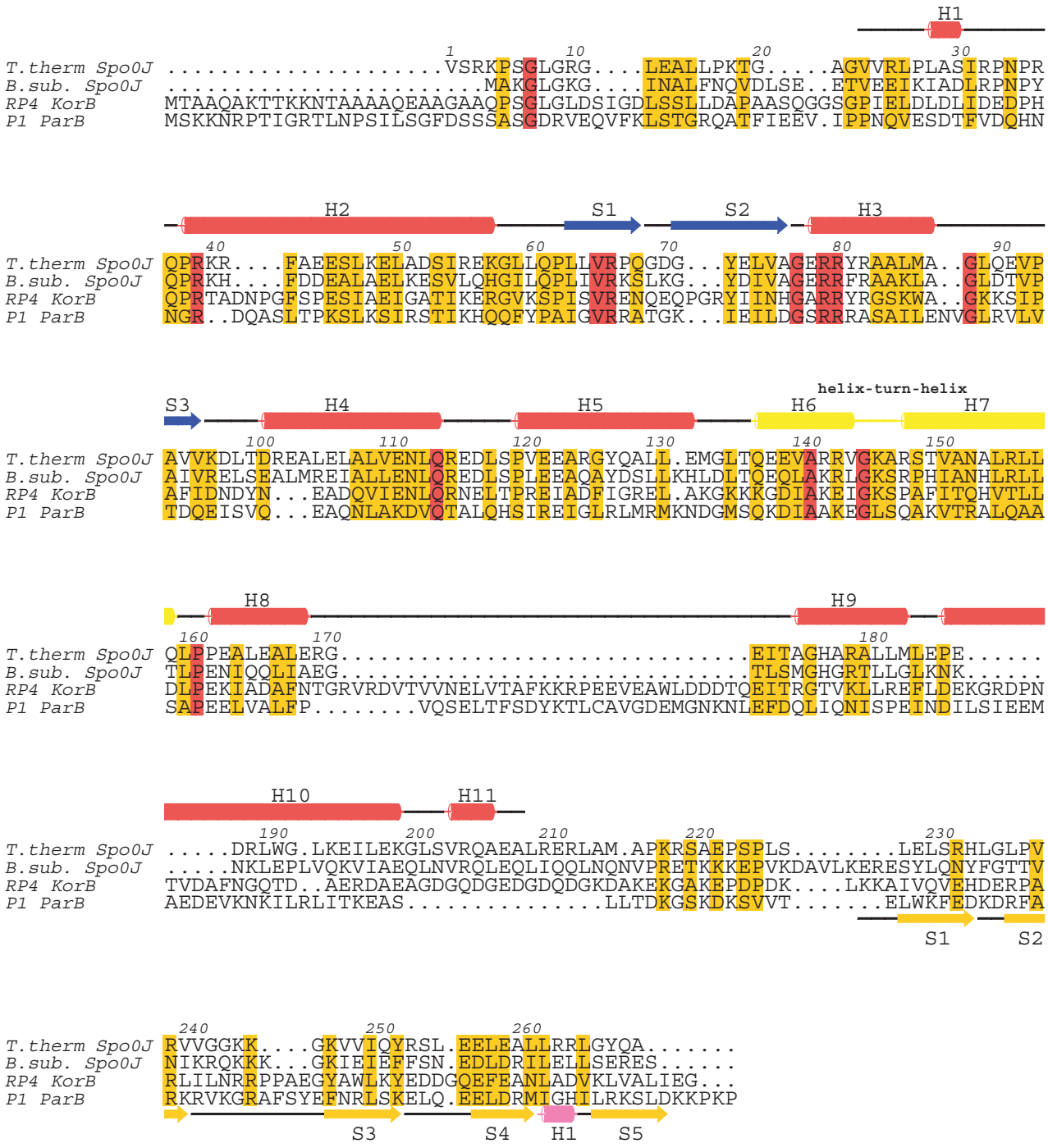

Fig. 6. Sequence alignment of the ParB proteins. Boundaries of the secondary structure elements were defined using the program DSSP (Kabsch and Sander, 1983). The colours of the secondary structure elements of Spo0J correspond to those of the domains shown in Fig. 2. The secondary structure of KorB–C (PDB entry 1IGQ) is shown below the alignment. Identical residues are coloured red, and conserved residues are coloured orange. The figure was prepared using the program ALSCRIPT (Barton, 1993).

which effectively increases the local concentration of the N-termini, facilitating dimerization; the second is that the C-terminus mediates dimerization of the full-length protein but that dimerization of the N-termini is dependent on DNA binding. Sedimentation velocity ultracentrifugation of the terminal 47 amino acids of Spo0J clearly shows it to be exclusively dimeric in solution (Fig. 5), an observation that is consistent with it forming a strong dimer structurally analogous to KorB–C. It is surprising that full-length Spo0J appears not to form as strong a dimer in solution

as the C-terminus alone: we speculate that dimerization of the N-termini is dependent on DNA binding. In the absence of DNA, the N-terminal domains are not dimerized and are partially inhibitory to strong dimerization of the C-terminus. This is reflected in the equilibrium dissociation constant of 10 μM calculated for the full-length protein.

In view of the above findings, we suggest that the C-terminus of Spo0J, like KorB–C, is the primary dimerization determinant and that the N-terminal portion represents a secondary dimerization determinant that is necessary for binding to DNA. Gel retardation assays show that full-length protein binds *parS* oligonucleotides but that the C-terminus is necessary for shifting plasmid DNA containing a single *parS* site (Fig. 1). We speculate that this results from the dependency of the DNA-binding domain on the C-terminus to bring them into a suitable context and elevated local concentration for binding to DNA. The requirement of the C-terminus for binding extensively to plasmid DNA raises the intriguing possibility that the C-terminus plays a role in dimer–dimer interactions with neighbouring molecules on the DNA, which allows the protein to nucleate at a *parS* site and 'spread' along the DNA, thereby effectively coating it. The equilibrium dissociation constant of 10 μM for dimerization of the full-length protein suggests that the dimerization of the C-termini (exclusively dimeric in solution alone) can be destabilized by the presence of the DNA-binding domains. It is a distinct possibility that, once dimerized on the DNA, the C-terminus is able to dimerize as effectively with the C-terminus of a neighbouring Spo0J dimer. The observation of gene silencing by P1 ParB (Rodionov *et al*., 1999) lends further support to this notion. Furthermore, it has been demonstrated that the C-terminus of KorB is essential for its ability to repress at a distance and that KorB can form higher order oligomeric complexes on DNA, its binding promoted by sequences flanking the operator regions to which it binds (Jagura-Burdzy *et al*., 1999). Figure 7 illustrates our proposed model of the primary Spo0J dimer (Fig. 7A) and C-terminus-mediated 'coating' of DNA (Fig. 7B).

Oligomerization of ParB proteins has been reported for both P1 ParB and ParB of *Streptomyces coelicolor* (Jakimowicz *et al*., 2002), with various proposals for its role. In an analogous fashion to ParR-mediated pairing of plasmid R1, it has been speculated that P1 ParB mediates pairing of plasmids through the formation of a partition complex spanning two *parS* sites on separate plasmids (Edgar

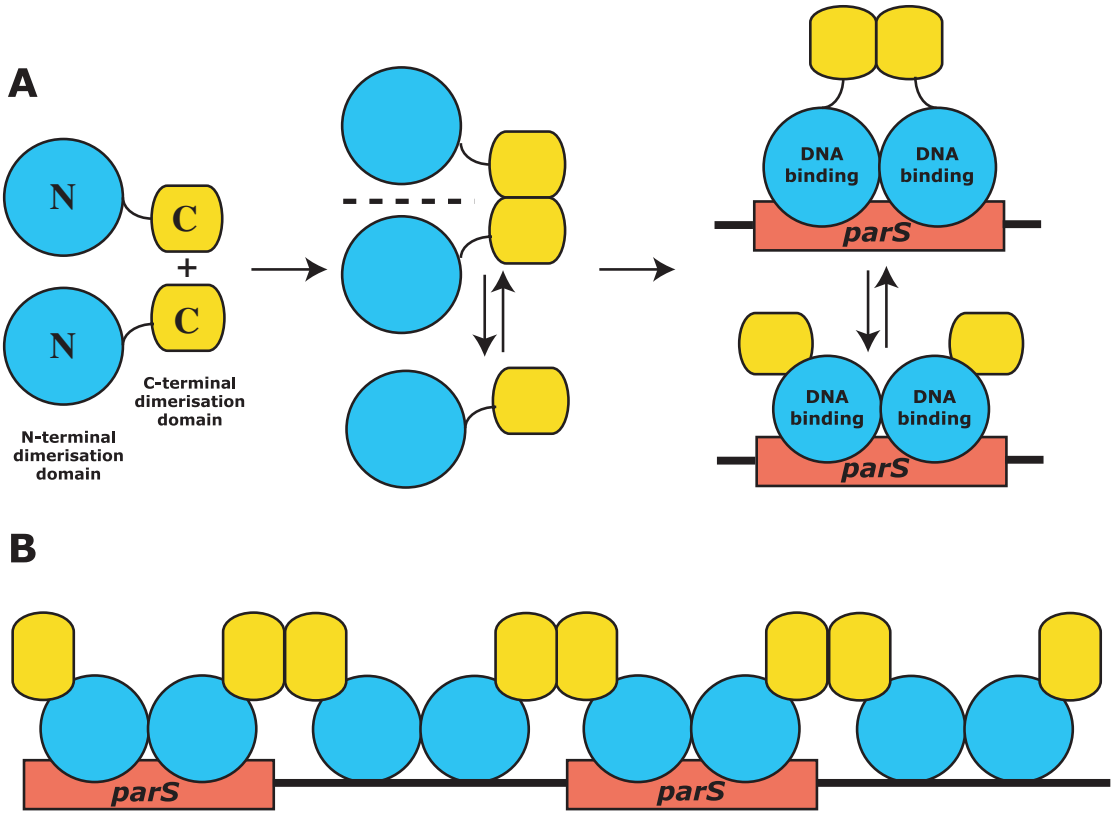

Fig. 7. Model of (A) the primary Spo0J dimer and (B) C-terminus-mediated 'coating' of DNA. The primary dimerization interface is located in the C-terminal region of Spo0J. The N-terminal/central portion forms a secondary dimerization domain that binds to DNA. Coating of DNA by Spo0J is dependent on the C-terminus.

et al., 2001). Others speculate that ParB forms a large nucleoprotein complex on *oriC* in which the DNA is wrapped around oligomers of ParB to form a compact nucleoprotein structure involved in DNA partitioning (Rodionov *et al*., 1999). The question of what happens when Spo0J binds to its cognate *parS* sites will clearly require further investigation.

Experimental procedures

Bacterial strains, media and culture conditions

Escherichia coli XL1-Blue served as host for all plasmid constructs. *E. coli* C41 (DE3) and C41 (BL21 DE3) RIL (*Codon plus*) were the hosts for overexpression of the Spo0J proteins. *E. coli* strains were grown on nutrient agar supplemented with ampicillin or chloramphenicol as desired and in 2× TY medium at 37°C until protein synthesis was induced at OD_{600} of 0.6 by the addition of 1 mM IPTG. Cells were then grown at 37°C for 5 h or 25°C overnight as required before harvesting. Ampicillin (100 μg ml^{-1}) and chloramphenicol (35 μg ml^{-1}) were added as required. Plasmids were introduced into *E. coli* by electroporation using electrocompetent cells.

Bacterial expression and protein purification

The polymerase chain reaction (PCR) was used to amplify the *spo0J* gene or constructs of the *spo0J* gene from the genomic DNA of various bacterial species. The forward primer was engineered to contain an *Nde*I restriction site at the start of the gene, and the reverse primer contained a *Bam*HI site in place of the stop codon at the end of the gene. The PCR fragments were digested with *Nde*I and *Bam*HI (3 h, 37°C) and cloned into the pHis17 vector, putting them under the control of the T7 promoter and adding eight residues at the C-terminus, which included a hexahistidine tag for affinity purification (GSHHHHHH). Spo0J1–222 from *T. thermophilus*, which was crystallized in this study, contains 230 residues and has a molecular weight of 25.4 kDa as confirmed by mass spectroscopy. C41 (DE3) RIL cells were transformed and expressed the His_6-tagged protein after the addition of IPTG (1 mM). For large-scale expression, 12 l of 2× TY medium containing 100 μg ml^{-1} ampicillin and 35 μg ml^{-1} chloramphenicol was inoculated from a 1:100 preculture and induced with 1 mM IPTG at OD_{600} = 0.6. Cells were harvested, frozen in liquid nitrogen and opened by sonication and the addition of lysozyme in 50 mM Tris, pH 7.4. The lysate was loaded onto a 10 ml Ni^{2+}-silica column, washed extensively with 50 mM Tris, 300 mM NaCl, 20 mM imidazole, pH 6.0. Protein was eluted with the same buffer containing 300 mM imidazole. The protein was diluted 10-fold in TEN (20 mM Tris, pH 7.5, 1 mM EDTA, 1 mM sodium azide) and applied to a 2× 5 ml HI-TRAP heparin (Amersham) column equilibrated in TEN. The protein was eluted in a linear gradient of 0–1 M NaCl in the same buffer. The protein was concentrated and applied to a Sephacryl S-200 column (Amersham) equilibrated in TEN + 5 mM $MgCl_2$. The protein was eluted as single peak and concentrated to 7.5 mg ml^{-1}. The protein can be stored at 4°C for several months.

The C-terminal domain of Spo0J (Spo0J223–269) was cloned using the vector pOPTM (O. Perisic, personal communication) and expressed as a hexahistidine-tagged protein fused to the C-terminus of the MalE fragment of maltose-binding protein (amino acids Met-1–Thr-367) with a linker containing a TEV protease cleavage site (sequence ASSSG-SENLYFQGSHM) between the two in C41 (DE3) cells. The fusion protein was purified by Ni^{2+}-NTA affinity chromatography according to the protocol used for the full-length and truncated proteins. The protein was buffer exchanged into 20 mM Tris, pH 8.5, 200 mM NaCl using a Sephadex G25 gel filtration column (Amersham). The eluate was concentrated to 10 mg ml^{-1} and incubated with TEV protease (O. Perisic, personal communication) at a ratio of 1 TEV:40 MalE-Spo0J223–269His_6 for 3 h at room temperature. The cleavage product GSHMSpo0J223–269His_6 was isolated by size exclusion on a Sephacryl S100 gel filtration column (Amersham).

Selenomethionine-substituted Spo0J

Selenomethionine (SeMet)-substituted protein was expressed in the C41 (DE3) RIL (*codon plus*) host, which is non-auxotrophic for methionine, and methionine biosynthesis was inhibited by the growth conditions (Van Duyne *et al*., 1993). A 1:1000 preculture in 2× TY medium was used to inoculate 250 ml of M9 minimal medium supplemented with 0.4% glucose, 2 mM $MgSO_4$, 100 μg ml^{-1} ampicillin, 35 μg ml^{-1} chloramphenicol, vitamins and trace elements. After growth overnight, the culture was diluted 1:50 into 12 l of minimal medium as above. After 10 h (OD_{600} = 0.3), 100 mg l^{-1} DL-selenomethionine (Fisher), 100 mg l^{-1} lysine, threonine and phenylalanine and 50 mg l^{-1} leucine, isoleucine and valine were added as solids. IPTG (1 mM) was added after 15 min, and cells were grown for 13 h (OD_{600} = 1.1). Methods of protein purification were identical to that for the unsubstituted protein with all Ni^{2+}-NTA buffers supplemented with 5 mM β-mercaptoethanol and all other buffers supplemented with 5 mM dithiothreitol (DTT).

Crystallization and data collection

Crystals were grown by the sitting drop vapour diffusion technique using 0.1 M sodium acetate, pH 4.0–5.0, 0.1–0.4 M KBr, 8% PEG550-MME, 8% PEG20K as the crystallization solution. Initial screens were performed using a Cartesian crystallization robot, which was set up to dispense 100 nl + 100 nl drops. A total of 1152 initial conditions were screened, and crystallization occurred under three very similar conditions. Droplets composed of one part 7.5 mg ml^{-1} protein solution and one part crystallization solution were equilibrated at 19°C for 1 week. Needle-like crystals grew from clear drops, and optimization of growth conditions failed to change the crystal morphology. Addition of 0.09 M hexamine cobalt trichloride facilitated the growth of single crystals belonging to space group C222. Crystals were soaked in cryobuffer containing 20–25% MPD and vitrified in liquid nitrogen. A native data set from a frozen crystal was collected

to 2.3 Å on ID14-4 at the ESRF, Grenoble, France. MAD data sets from a single selenomethionine-substituted crystal were also collected on ID14-4 at the ESRF.

Structure determination and refinement

All data were indexed and integrated with the MOSFLM package and processed further using the CCP4 suite of programs (Project, 1994). Identification of 35 selenium atoms was performed by SHAKE 'N' BAKE (Miller *et al*., 1994), and phasing was performed by SHARP (La Fortelle, 1997). Solvent flattening using 46% solvent produced an almost perfect electron density map. After initial model building, the non-crystallographic symmetry was determined as four dimers per asymmetric unit. Averaging and phase extension yielded a final experimental map at 2.3 Å resolution. All four dimers of Spo0J were built using MAIN and refined using CNS with Engh and Huber stereochemical parameters (Engh, 1991). Details of the final model are summarized in Table 2.

Analytical sedimentation

Sedimentation equilibrium and velocity experiments were performed in a Beckman Optima XL-A analytical ultracentrifuge with an An60-Ti rotor, with the sample in various buffers as described in the text.

Velocity

Sedimentation velocity was at 60 000 rev min^{-1}, 20.0°C, with scans of the single cell taken at 0 min intervals (to obtain scans as closely spaced as possible) or 2.5 min intervals. Adjacent sets of data (up to 12 scans, but fewer when this many would give broadening) were analysed by the method of Stafford (1994, 1997) using the program DCDT+ (Philo, 2000).

Equilibrium

Sedimentation equilibrium was typically performed at 10 000 or 15 000 rev min^{-1}, 20.0°C, with initial overspeeding 50% faster for 6 h to reduce the time to reach equilibrium (Van Holde and Baldwin, 1958). Long sample columns were used, with cells loaded at a variety of initial concentrations. Scans (averaging 10 readings) were taken at 230 nm at 24 h intervals until no movement of the distribution was visible, when final scans (averaging 100 readings) were taken and assumed to be operationally at equilibrium. The rotor was then accelerated to pull the macromolecule away from the meniscus, and further scans were taken to provide initial estimates of the baseline for each cell.

Measurement of density increments and extinction coefficients

The density increment $\left[\left(\frac{\partial \rho}{\partial c_2}\right)_\mu\right]$ for the macromolecule (component 2), at constant chemical potential of water (component 1) and all diffusible solutes (components 3), at 5.0°C in 20 mM Tris, pH 7.5, 150 mM NaCl, 5 mM $MgSO_4$ was calculated directly from the difference in densities of a solution of the macromolecule and the solvent, where the solution was at dialysis equilibrium with the solvent. The densities of both the buffer and the solution were measured with a DMA 60 digital density meter, with a DMA 602 measuring cell (Anton Paar) (Kratky *et al*., 1973) The concentration of the macromolecule (c_2) was measured for the protein alone by amino acid analysis.

The solvent density and viscosity, at different temperatures and for buffers of different composition, were calculated using the program SEDNTERP (Laue *et al*., 1992).

Spectra were plotted for the sample solutions, used for measurements of the densities, enabling appropriate extinction coefficients to be calculated using the protein concentrations determined from the amino acid analyses.

DNA-binding assays

A 16 bp DNA fragment containing the Spo0J binding site from *B. subtilis* (Lin and Grossman, 1998) was used as the probe in gel mobility shift assays. Two oligonucleotides, 5′-TGTTC CACGTGAAACA-3′ and its complement 5′-TGTTTCACGTG GAACA-3′, were annealed by heating an equimolar mixture of the complementary single-stranded oligonucleotides at 99°C for 10 min and cooling to room temperature overnight. Binding reactions were performed in a volume of 10 μl in 20 mM Tris-HCl, pH 8.0, 5 mM $MgSO_4$. Each reaction contained 300 μM *parS* DNA and 0–300 μM purified, hexahistidine-tagged Spo0J. The reactions were incubated at 25°C for 20 min, mixed with gel loading buffer and run on a 1% agarose gel in 0.5× TB buffer. For gel retardation of plasmid DNA containing a single *parS* site, 2.8 pmol of a pUC19 derivative plasmid, pUOJ (H. Ferreira, personal communication), engineered to contain a single *parS* site, was incubated with 0–1000 pmol of full-length Spo0J and Spo0J1–222 in 20 mM Tris, pH 8.0, 100 mM NaCl, 5 mM $MgSO_4$ at 25°C for 20 min. Gels were stained with ethidium bromide and visualized on a UV transilluminator.

Acknowledgements

We thank Steffi Arzt at beamline ID-14-4, ESRF (Grenoble) for assistance with data collection, and Sew Peak-Chew (MRC-LMB, Cambridge) for performing N-terminal sequencing and mass spectroscopy. We thank Olga Perisic for providing us with the pOPTM vector and TEV protease. We also thank Jeff Errington and Henrique Ferreira (Oxford) for useful discussions and for providing plasmid pUOJ.

References

Austin, S., and Abeles, A. (1983a) Partition of unit-copy miniplasmids to daughter cells. I. P1 and F miniplasmids contain discrete, interchangeable sequences sufficient to promote equipartition. *J Mol Biol* **169:** 353–372.

Austin, S., and Abeles, A. (1983b) Partition of unit-copy miniplasmids to daughter cells. II. The partition region of miniplasmid P1 encodes an essential protein and a centromere-like site at which it acts. *J Mol Biol* **169:** 373–387.

Autret, S., Nair, R., and Errington, J. (2001) Genetic analysis of the chromosome segregation protein Spo0J of *Bacillus*

subtilis: evidence for separate domains involved in DNA binding and interactions with Soj protein. *Mol Microbiol* **41:** 743–755.

Balzer, D., Ziegelin, G., Pansegrau, W., Kruft, V., and Lanka, E. (1992) KorB protein of promiscuous plasmid RP4 recognizes inverted sequence repetitions in regions essential for conjugative plasmid transfer. *Nucleic Acids Res* **20:** 1851–1858.

Barton, G.J. (1993) ALSCRIPT: a tool to format multiple sequence alignments. *Protein Eng* **6:** 37–40.

Bouet, J.Y., Surtees, J.A., and Funnell, B.E. (2000) Stoichiometry of P1 plasmid partition complexes. *J Biol Chem* **275:** 8213–8219.

Delbruck, H., Ziegelin, G., Lanka, E., and Heinemann, U. (2002) An Src homology 3-like domain is responsible for dimerization of the repressor protein KorB encoded by the promiscuous IncP plasmid RP4. *J Biol Chem* **277:** 4191–4198.

Dworkin, J., and Losick, R. (2002) Does RNA polymerase help drive chromosome segregation in bacteria? *Proc Natl Acad Sci USA* **99:** 14089–14094.

Edgar, R., Chattoraj, D.K., and Yarmolinsky, M. (2001) Pairing of P1 plasmid partition sites by ParB. *Mol Microbiol* **42:** 1363–1370.

Engh, R.A.H. (1991) Accurate bond and angle parameters for X-ray protein structure refinement. *Acta Crystallogr Sect A* **47:** 392–400.

van den Ent, F., Moller-Jensen, J., Amos, L.A., Gerdes, K., and Lowe, J. (2002) F-actin-like filaments formed by plasmid segregation protein ParM. *EMBO J* **21:** 6935–6943.

Gerdes, K., Moller-Jensen, J., and Bugge Jensen, R. (2000) Plasmid and chromosome partitioning: surprises from phylogeny. *Mol Microbiol* **37:** 455–466.

Godfrin-Estevenon, A.M., Pasta, F., and Lane, D. (2002) The parAB gene products of *Pseudomonas putida* exhibit partition activity in both *P. putida* and *Escherichia coli*. *Mol Microbiol* **43:** 39–49.

Gordon, G.S., and Wright, A. (2000) DNA segregation in bacteria. *Annu Rev Microbiol* **54:** 681–708.

Gordon, G.S., Sitnikov, D., Webb, C.D., Teleman, A., Straight, A., Losick, R., *et al.* (1997) Chromosome and low copy plasmid segregation in *E. coli*: visual evidence for distinct mechanisms. *Cell* **90:** 1113–1121.

Gough, J., Karplus, K., Hughey, R., and Chothia, C. (2001) Assignment of homology to genome sequences using a library of hidden Markov models that represent all proteins of known structure. *J Mol Biol* **313:** 903–919.

Hayes, F. (2000) The partition system of multidrug resistance plasmid TP228 includes a novel protein that epitomizes an evolutionarily distinct subgroup of the ParA superfamily. *Mol Microbiol* **37:** 528–541.

Heald, R. (2000) Motor function in the mitotic spindle. *Cell* **102:** 399–402.

Hiraga, S. (2000) Dynamic localization of bacterial and plasmid chromosomes. *Annu Rev Genet* **34:** 21–59.

Holm, L., and Sander, C. (1995) Dali: a network tool for protein structure comparison. *Trends Biochem Sci* **20:** 478–480.

Ireton, K., Gunther, N.W.T., and Grossman, A.D. (1994) spo0J is required for normal chromosome segregation as well as the initiation of sporulation in *Bacillus subtilis*. *J Bacteriol* **176:** 5320–5329.

Jacob, F., Brenner, S., and Cuzin, F. (1963) On the regulation of DNA replication in bacteria. *Cold Spring Harbor Symp Quant Biol* **23:** 329–348.

Jagura-Burdzy, G., Macartney, D.P., Zatyka, M., Cunliffe, L., Cooke, D., Huggins, C., *et al.* (1999) Repression at a distance by the global regulator KorB of promiscuous IncP plasmids. *Mol Microbiol* **32:** 519–532.

Jakimowicz, D., Chater, K., and Zakrzewska-Czerwinska, J. (2002) The ParB protein of *Streptomyces coelicolor* A3(2) recognizes a cluster of parS sequences within the origin-proximal region of the linear chromosome. *Mol Microbiol* **45:** 1365–1377.

Jensen, R.B., and Gerdes, K. (1999) Mechanism of DNA segregation in prokaryotes: ParM partitioning protein of plasmid R1 co-localizes with its replicon during the cell cycle. *EMBO J* **18:** 4076–4084.

Jensen, R.B., and Shapiro, L. (1999) The *Caulobacter crescentus* smc gene is required for cell cycle progression and chromosome segregation. *Proc Natl Acad Sci USA* **96:** 10661–10666.

Kabsch, W., and Sander, C. (1983) Dictionary of protein secondary structure: pattern recognition of hydrogen-bonded and geometrical features. *Biopolymers* **22:** 2577–2637.

Konig, P., Giraldo, R., Chapman, L., and Rhodes, D. (1996) The crystal structure of the DNA-binding domain of yeast RAP1 in complex with telomeric DNA. *Cell* **85:** 125–136.

Koppes, L.J., Woldringh, C.L., and Nanninga, N. (1999) *Escherichia coli* contains a DNA replication compartment in the cell center. *Biochimie* **81:** 803–810.

Kratky, O., Leopold, H., and Stabinger, H. (1973) The determination of the partial specific volume of proteins by the mechanical oscillator technique. *Methods Enzymol* **27:** 98–110.

Kraulis, P.J. (1991) MOLSCRIPT: a program to produce both detailed and schematic plots of protein structures. *J Appl Crystallogr* **24:** 946–950.

La Fortelle, E.D.B. (1997) *Methods in Enzymology, 276. Macromolecular Crystallography.* New York: Academic Press, pp. 472–494.

Laskowski, R.A., Moss, D.S., and Thornton, J.M. (1993) Main-chain bond lengths and bond angles in protein structures. *J Mol Biol* **231:** 1049–1067.

Laue, T.M., Shah, B.D., Ridgeway, T.M., and Pelletier, S.L. (1992) Computer-aided interpretation of analytical sedimentation data for proteins. In *Analytical Ultracentrifugation in Biochemistry and Polymer Science*. Horton, J.C. (ed.). Cambridge: Royal Society of Chemistry, pp. 90–125.

Lemon, K.P., and Grossman, A.D. (1998) Localization of bacterial DNA polymerase: evidence for a factory model of replication. *Science* **282:** 1516–1519.

Lemon, K.P., and Grossman, A.D. (2000) Movement of replicating DNA through a stationary replisome. *Mol Cell* **6:** 1321–1330.

Lemon, K.P., and Grossman, A.D. (2001) The extrusion-capture model for chromosome partitioning in bacteria. *Genes Dev* **15:** 2031–2041.

Lewis, P.J., and Errington, J. (1997) Direct evidence for active segregation of oriC regions of the *Bacillus subtilis*

chromosome and co-localization with the SpoOJ partitioning protein. *Mol Microbiol* **25:** 945–954.
Lewis, R.A., Bignell, C.R., Zeng, W., Jones, A.C., and Thomas, C.M. (2002) Chromosome loss from par mutants of *Pseudomonas putida* depends on growth medium and phase of growth. *Microbiology* **148:** 537–548.
Lin, D.C., and Grossman, A.D. (1998) Identification and characterization of a bacterial chromosome partitioning site. *Cell* **92:** 675–685.
Luscombe, N.M., Austin, S.E., Berman, H.M., and Thornton, J.M. (2000) An overview of the structures of protein-DNA complexes. *Genome Biol* **1:** REVIEWS001.
Miller, R., Gallo, S.M., Khalak, H.G., and Weeks, C.M. (1994) SnB – crystal-structure determination via shake-and-bake. *J Appl Crystallog* **27:** 613–621.
Mobley, H.L., Koch, A.L., Doyle, R.J., and Streips, U.N. (1984) Insertion and fate of the cell wall in *Bacillus subtilis*. *J Bacteriol* **158:** 169–179.
Mohl, D.A., Easter, J., Jr, and Gober, J.W. (2001) The chromosome partitioning protein, ParB, is required for cytokinesis in *Caulobacter crescentus*. *Mol Microbiol* **42:** 741–755.
Moller-Jensen, J., Jensen, R.B., and Gerdes, K. (2000) Plasmid and chromosome segregation in prokaryotes. *Trends Microbiol* **8:** 313–320.
Nardmann, J., and Messer, W. (2000) Identification and characterization of the dnaA upstream region of *Thermus thermophilus*. *Gene* **261:** 299–303.
Nicholls (1993) *GRASP: Graphical Representation and Analysis of Surface Properties*. New York: Columbia University.
Niki, H., and Hiraga, S. (1997) Subcellular distribution of actively partitioning F plasmid during the cell division cycle in *E. coli*. *Cell* **90:** 951–957.
Niki, H., and Hiraga, S. (1998) Polar localization of the replication origin and terminus in *Escherichia coli* nucleoids during chromosome partitioning. *Genes Dev* **12:** 1036–1045.
Niki, H., Yamaichi, Y., and Hiraga, S. (2000) Dynamic organization of chromosomal DNA in *Escherichia coli*. *Genes Dev* **14:** 212–223.
Onogi, T., Ohsumi, K., Katayama, T., and Hiraga, S. (2002) Replication-dependent recruitment of the beta-subunit of DNA polymerase III from cytosolic spaces to replication forks in *Escherichia coli*. *J Bacteriol* **184:** 867–870.
Pabo, C.O., and Lewis, M. (1982) The operator-binding domain of lambda repressor: structure and DNA recognition. *Nature* **298:** 443–447.
Pabo, C.O., and Sauer, R.T. (1992) Transcription factors: structural families and principles of DNA recognition. *Annu Rev Biochem* **61:** 1053–1095.
Philo, J.S. (2000) A method for directly fitting the time derivative of sedimentation velocity data and an alternative algorithm for calculating sedimentation coefficient distribution functions. *Anal Biochem* **279:** 151–163.
Project, C.C. (1994) The CCP4 suite: programs for protein crystallography. *Acta Crystallogr D* **50:** 760–763.
Rodionov, O., Lobocka, M., and Yarmolinsky, M. (1999) Silencing of genes flanking the P1 plasmid centromere. *Science* **283:** 546–549.
Sawitzke, J., and Austin, S. (2001) An analysis of the factory model for chromosome replication and segregation in bacteria. *Mol Microbiol* **40:** 786–794.
Sharp, D.J., Rogers, G.C., and Scholey, J.M. (2000) Microtubule motors in mitosis. *Nature* **407:** 41–47.
Sharpe, M.E., and Errington, J. (1996) The *Bacillus subtilis* soj-spo0J locus is required for a centromere-like function involved in prespore chromosome partitioning. *Mol Microbiol* **21:** 501–509.
Sharpe, M.E., and Errington, J. (1999) Upheaval in the bacterial nucleoid. An active chromosome segregation mechanism. *Trends Genet* **15:** 70–74.
Stafford, W.F., III (1994) Methods for obtaining sedimentation coefficient distributions. In *Analytical Ultracentrifugation in Biochemistry and Polymer Science*. Horton, J.C. (ed.). Cambridge: The Royal Society of Chemistry, pp. 359–393.
Stafford, W.F., III (1997) Sedimentation velocity spins a new weave for an old fabric. *Curr Opin Biotechnol* **8:** 14–24.
Surtees, J.A., and Funnell, B.E. (2001) The DNA binding domains of P1 ParB and the architecture of the P1 plasmid partition complex. *J Biol Chem* **276:** 12385–12394.
Suzuki, M., Yagi, N., and Gerstein, M. (1995) DNA recognition and superstructure formation by helix-turn-helix proteins. *Protein Eng* **8:** 329–338.
Van Duyne, G.D., Standaert, R.F., Karplus, P.A., Schreiber, S.L., and Clardy, J. (1993) Atomic structures of the human immunophilin FKBP-12 complexes with FK506 and rapamycin. *J Mol Biol* **229:** 105–124.
Van Holde, K.E., and Baldwin, R.L. (1958) Rapid attainment of sedimentation equilibrium. *J Phys Chem* **62:** 734–743.
Webb, C.D., Teleman, A., Gordon, S., Straight, A., Belmont, A., Lin, D.C., *et al.* (1997) Bipolar localization of the replication origin regions of chromosomes in vegetative and sporulating cells of *B. subtilis*. *Cell* **88:** 667–674.
Webb, C.D., Graumann, P.L., Kahana, J.A., Teleman, A.A., Silver, P.A., and Losick, R. (1998) Use of time-lapse microscopy to visualize rapid movement of the replication origin region of the chromosome during the cell cycle in *Bacillus subtilis*. *Mol Microbiol* **28:** 883–892.
Wheeler, R.T., and Shapiro, L. (1997) Bacterial chromosome segregation: is there a mitotic apparatus? *Cell* **88:** 577–579.
Yamaichi, Y., and Niki, H. (2000) Active segregation by the *Bacillus subtilis* partitioning system in *Escherichia coli*. *Proc Natl Acad Sci USA* **97:** 14656–14661.
Yamaichi, Y., and Niki, H. (2004) migS, a cis-acting site that affects bipolar positioning of oriC on the *Escherichia coli* chromosome. *EMBO J* **23:** 221–233.